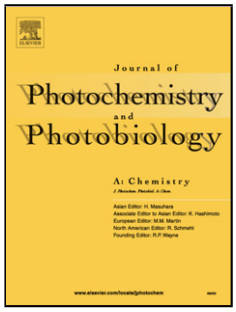

Title: A FRET based colorimetric and fluorescence probe for selective detection of Bi^{3+} ion and live cell imaging

Authors: Susanta Adhikari, Sandip Mandal, Avijit Ghosh, Subhajit Guria, Abhishek Pal, Arghya Adhikary, Debasis Das

PII: S1010-6030(18)30133-3
DOI: https://doi.org/10.1016/j.jphotochem.2018.04.005
Reference: JPC 11220

To appear in: *Journal of Photochemistry and Photobiology A: Chemistry*

Received date: 30-1-2018
Revised date: 31-3-2018
Accepted date: 3-4-2018

Please cite this article as: Susanta Adhikari, Sandip Mandal, Avijit Ghosh, Subhajit Guria, Abhishek Pal, Arghya Adhikary, Debasis Das, A FRET based colorimetric and fluorescence probe for selective detection of Bi3+ ion and live cell imaging, Journal of Photochemistry and Photobiology A: Chemistry https://doi.org/10.1016/j.jphotochem.2018.04.005

A FRET based colorimetric and fluorescence probe for selective detection of Bi^{3+} ion and live cell imaging

Susanta Adhikari[a*], Sandip Mandal[b], Avijit Ghosh[a,c], Subhajit Guria[a], Abhishek Pal[a], Arghya Adhikary[c] and Debasis Das[b*]

[a]Department of Chemistry, University of Calcutta, 92, A.P.C. Road, Kolkata 700 009, West Bengal, India., E-mail address: *adhikarisusanta@yahoo.com*

[b]Department of Chemistry, The University of Burdwan, 713104, Burdwan, West Bengal, India. E-mail: *ddas100in@yahoo .com*

[c]Centre for Research in Nanoscience & Nanotechnology, (CRNN), University of Calcutta, Technology Campus, Sector-III, Block-JD2, Salt Lake, Kolkata 700098, West Bengal,India

Graphical abstract

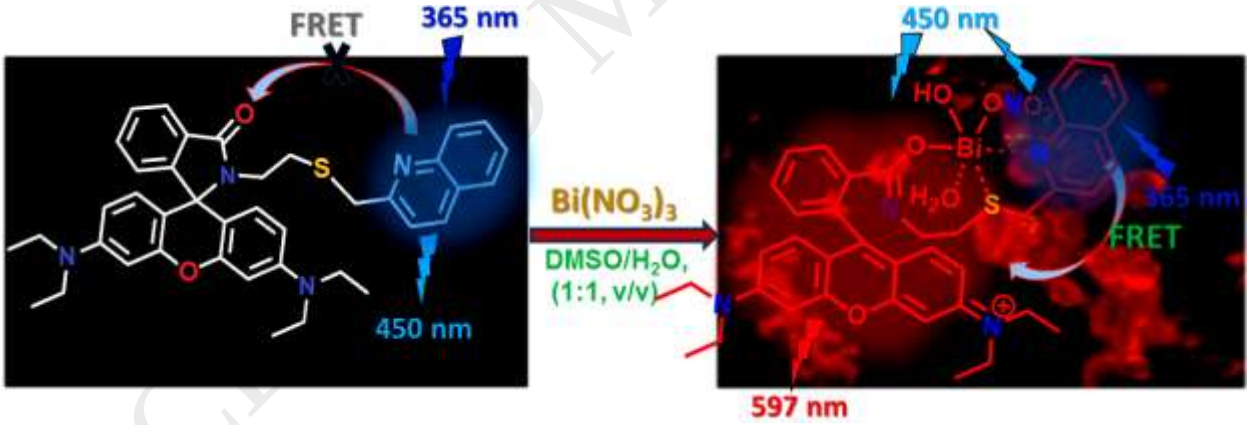

Highlights

1. A Rhodamine B-Quinoline conjugate (RSQ) selectively detects Bi^{3+} by colorimetric and fluorescence methods.
2. RSQ detects Bi^{3+} as low as 0.05 µM.
3. The sensing mechanism is based on CHEF assisted FRET process.
4. RSQ efficiently images intracellular Bi^{3+} in SiHa live cells.

Abstract: A Rhodamine B- quinoline conjugate (**RSQ**) functions as a colorimetric and fluorescence probe for selective recognition of Bi^{3+} ion based on CHEF assisted FRET process. **RSQ** visibly changes its colour and fluorescence profile upon addition of Bi^{3+} ion. The distinctive colour change allows facile discrimination of Bi^{3+} over other common cations. Lowest concentration of Bi^{3+} detected by **RSQ** is 0.05 μM. **RSQ** efficiently images intracellular Bi^{3+} in live SiHa cells.

Keywords: Rhodamine-quinoline conjugate • Solvent dependent selectivity and sensitivity • DFT calculation • Live cell imaging

1. Introduction

Use of bismuth in semiconductors[1], cosmetic products (in pigment for eye shadow, lipstick and hair dye)[2], medicines (for treatment of syphilis, peptic ulcers, hypertension and dermatological disorders)[3], alloys, catalysts[4], metallurgical additives and preparation and recycling of uranium in nuclear fuels[5] is continuously increasing bismuth exposure to human beings. Traces of Bi may alter physical, mechanical and magnetic properties of metallurgical materials.[6]

Food and Agricultural Organization (FAO) and World Health Organization (WHO) do not recommend bismuth as a trace level essential element, although several bismuth compounds have numerous medicinal applications. Nevertheless, the mechanisms of biological activities are not well established.[7]

The toxicity of Bi found in human and other animals includes osteo-arthopathy, hepatitis and neuropathology, encephalopathy and nephrotoxicity.[5] Oral intake of Bi compounds by mice may lead its accumulation in nervous system (particularly in motor neurons)[8]. Chronic exposure to Bi causes its aggregation at epithelial cells, leading to characteristic intra-cytoplasmic inclusions. The absorbed Bi is transported *via* human serum to the cells, and finally excreted through urine.

Several methods are available for determination of traces of Bi, *viz.* electro thermal atomic absorption spectrometry (ET-AAS),[9] inductively coupled plasma mass spectrometry (ICP-MS),[10] hydride generation atomic absorption/fluorescence spectrometry,[11] spectrophotometry[12] and light scattering technique.[13] However, they involve several drawbacks like expensive instrumentation, use of toxic organic solvents and requires pre-concentration/ separation. Stripping voltammetry also allows selective determination of Bi[14].However, use of toxic mercury salts and electrodes, and presence of overlapping peaks of Bi^{3+} and Cu^{2+} are two serious limitations of this process.

Fluorescence based optical sensors have been emerged as valuable tools to overcome those drawbacks. This technique involves very fast response, simple procedure and non-invasive method allowing applications to varieties physiological systems.

Lack of Bi^{3+} selective chemo-sensor inspired us to develop rhodamine B-quinoline conjugate,3',6'-bis(diethylamino)-2-(2-((quinolin-2-ylmethyl)thio)ethyl)spiro[isoindoline-1,9'-xanthen]-3-one (**RSQ**). We have not found any Bi^{3+} selective fluorescence probe in literature that functions through FRET mechanism in 1:1 DMSO: water (v/v). Rhodamine based probes are well known for red light emission, high quantum yield, low back ground emission, low cytotoxicity, cell permeability, and good fluorescence resonance energy transfer (FRET) acceptor.[15] **RSQ** visibly changes its colour and fluorescence profile upon addition of Bi^{3+} ion that allows facile discrimination over other common cations.

2. Experimental

2.1. Materials and equipment

Chemicals and solvents were purchased from commercial suppliers and used as received. ^{1}H and ^{13}C NMR spectra were recorded on a Bruker Advance III HD (300 MHz) spectrometer. Chemical shifts were reported in parts per million (ppm), and the residual solvent peak was used as an internal reference: proton (chloroform δ 7.26), carbon (chloroform δ 77.16) or tetramethylsilane (TMS δ 0.00) was used as a reference. Multiplicity was indicated as follows: s (singlet), d (doublet), t (triplet), q (quartet), m (multiplet). Coupling constants were reported in Hertz (Hz). High resolution mass spectra were obtained on a Micro mass/Q-Toff. micro™ spectrometer. For thin layer chromatography (TLC), Merck precoated TLC plates (Merck 60 F254) were used and flash chromatography separations were performed on SRL 230-400 mesh silica gel.

2.2. General method of UV-Vis and fluorescence titration

Path length of the cells used for absorption and emission studies was 1 cm. For UV-Vis. and fluorescence titrations, stock solution of **RSQ** (10 μM) was prepared in DMSO/water (1/1, v/v) using HEPES (0.1M, pH 7.4) buffer. Working solutions of **RSQ** and Bi^{3+} were prepared from their respective stock solutions. Fluorescence measurements were performed using 5 nm x 5 nm slit width. Except time dependent spectra, all the fluorescence and absorbance spectra were taken after 5 minutes of mixing of analyte to **RSQ**.

2.3. Calculation of Quantum Yield

Fluorescence quantum yields (Φ) were estimated by integrating the area under the fluorescence curves using the equation,

Where **A** was the area under the fluorescence spectral curve and **OD** was optical density of the compound at the excitation wavelength. The standard used for the measurement of fluorescence quantum yield was rhodamine-B (Φ = 0.7 in ethanol). The area of the emission spectrum was integrated using the software available in the instrument and the quantum yield was calculated according to the equation.

2.4. Job's plot from fluorescence experiments

A series of solutions containing **RSQ** and Bi^{3+} were prepared in such a way that the total concentration of Bi^{3+} and **RSQ** remain constant (10 μM) in all the sets. The mole fraction (X) of **RSQ** was varied from 0.1 to 0.9. The emission intensity at 597 nm was plotted against the mole fraction of the ligand (**RSQ**) in solution.

2.5. Synthesis

2.5.1. Synthesis of 2-(bromomethyl) quinolone (1)

2-(Bromomethyl) quinolone was prepared according to the literature procedure[16, 17a-b]. Selective bromination of the 2-methyl quinoline (3.0 g, 32.2 mmol) with 1.5 equivalents of NBS in CCl_4 for 12 hours afforded 1.3 g of compound **1** in 23.2% yield as yellow solid. The solid was characterized by ^{1}H NMR (Figure S-1) (300 MHz, in ppm $CDCl_3$): δ 8.187-8.159 (d, J = 8.4 Hz, 1H), 8.104-8.076 (d, J= 8.4 Hz, 1H), 7.832-7.804 (d, J = 8.4 Hz, 1H), 7.770-7.714 (m,1H), 7.589-7.538 (t, J= 8.4 Hz, 2H), 4.730 (s, 2H). ^{13}C NMR (Figure S-2) (75 MHz, $CDCl_3$): δ 156.86, 147.50, 137.25, 129.92, 129.25, 127.50, 127.43, 127.31, 127.00, 121.13, 34.37.

2.5.2. Synthesis of 2-((quinolin-2-ylmethyl)thio)ethan-1-amine (2)

A mixture of 2-(bromomethyl) quinoline(1.3 g, 7.55 mmol) and 2-amino-ethanethiol (581 mg, 7.55 mmol) in dry ethanol (10 mL), was added to a *in-situ* solution of sodium ethanolate, prepared by mixing sodium (166.42 mg, 7.23 mmol) to dry ethanol (15 mL) under nitrogen. The mixture was stirred for 5 h at room temperature. After completion of the reaction as monitored by TLC, the mixture was neutralized and extracted with ethyl acetate. The crude product was isolated by flash chromatography on silica gel using MeOH/ DCM (1:9, v/v) to get yellow liquid, assigned as **2** with 65% yield (824 mg,). The liquid was characterized by ^{1}H NMR (Figure S-3) (300 MHz, $CDCl_3$): δ = 1.521 (2H, s), 2.265 (2H, t), 2.505 (2H, t), 3.665 (2H, s), 7.163 (2H, m), 7.361 (2H, m), 7.742 (2H, m). ^{13}C NMR (Figure S-4) (75 MHz, $CDCl_3$): δ 158.49, 146.91, 136.51, 129.23, 128.89, 128.44, 127.17, 127.10, 127.03, 126.63, 126.56, 126.49, 126.43, 125.92, 121.50, 120.76, 39.86, 37.81, 30.44.

2.5.3. Synthesis of 3', 6'-bis(diethylamino)-2-(2-((quinolin-2-ylmethyl)thio)ethyl)spiro[isoindoline-1,9'-xanthen]-3-one (RSQ)

The acid chloride of rhodamine[17(c)] in DCE (479 mg, 1 mmol) was added to the stirred solution of amine, 2 (168 mg, 1 mmol) in DCE in presence of few drops of triethyl amine. The reaction mixture was refluxed for 6 h. Upon completion of the reaction as monitored by TLC, the solvent was removed in

vacuum to dryness. The reaction mixture was treated with water, extracted with ethyl acetate, and dried over anhydrous Na_2SO_4. The organic layer was removed under reduced pressure and the residue was purified by column chromatography (EtOAc/ hexane, 3:7, v/v) to yield pink solid (290 mg, 45%), RSQ.

The solid was characterized by ^{1}H NMR (Figure S-5) (300 MHz, $CDCl_3$):δ = 1.167 (12H, t), 2.163 (2H, t), 2.310 (2H, t), 3.435 (8H, m), 4.106 (2H, s), 6.253 (2H, s), 6.350 (2H, d), 6.442 (2H, d), 7.067 (1H, d), 7.395-7.497 (3H, m), 7.656-7.760 (3H, m), 7.933 (1H, d), 8.035 (1H, m), 8.075 (1H, m); ^{13}C NMR (Figure S-6) (75 MHz, $CDCl_3$) δ = 12.43, 29.31, 29.83, 38.07, 39.48, 43.97, 60.00, 64.43, 97.42, 105.15, 107.78, 120.99, 122.45, 123.4, 125.73, 126.64, 127.03, 127.64, 128.51, 128.79, 129.01, 130.75, 132.03, 136.25, 147.46, 148.48, 152.91, 153.21, 158.62, 167.64; and QTOF mass (Figure S-5) m/z $(M+H)^+$ calculated for $C_{40}H_{43}N_4O_2S^+$ is 643.3101, found: 643.3149.

2.5.4. Synthesis of N-(2-((quinolin-2-ylmethyl)thio)ethyl)acetamide (3)

To dichloromethane solution of **2** (218 mg, 1 mmol), acetic anhydride (204 mg, 2 mmol) was added under stirring condition in presence of few drops of triethylamine. The reaction mixture was stirred for 6 h. Upon completion of the reaction as monitored by TLC, the solvent was removed in vacuum. The residue was partitioned and extracted with ethyl acetate from water and dried over anhydrous Na_2SO_4. The organic layer was removed under reduced pressure and the residue was purified by column chromatography (EtOAc/ hexane, 3:7, v/v) to yield 170 mg (65%) of 3 as a yellow liquid.

^{1}H NMR (300 MHz, $CDCl_3$) (Figure S-7): *δ,* 8.075-8.046 (d , *J* = 8.7 Hz, 1H), 7.981-7.953 (d, *J* = 8.4 Hz, 1H), 7.737-7.710 (d, *J* = 8.1 Hz, 1H), 7.652-7.601 (m,1H), 7.474-7.415 (m, 2H), 3.943 (s, 2H), 3.433-3.373 (q, *J* = 5.7Hz, 2H), 2.588-2.546 (t, J = 6.3 Hz, 2H), 1.901 (s, 3H). ^{13}C NMR (75 MHz, $CDCl_3$) (Figure S-8): *δ,* 170.29, 158.75, 147.22, 137.10, 129.71, 128.63, 127.56, 126.96, 126.41, 121.23, 39.18, 37.96, 30.87, 23.06.

3. Results and discussion

Bi^{3+} has thiophilic character and thus has affinity for S-donors leading to the formation of thermodynamically stable Bi-S bond.[18]In our designed probe RSQ, we have carefully combined quinoline and rhodamine moieties through a flexible 'S' donor spacer (Scheme 1). Previously, we have designed Au^{3+} selective probe having N, O and S donor sites based on rhodamine-quinoline conjugate.[16]The selectivity of rhodamine based probes can be tuned through variation of spacer and relative orientation of donor sites. Generally, rhodamine based probes are selective for Al^{3+}, Cu^{2+}, Hg^{2+}, Fe^{3+} or Cr^{3+} ions[19] while 'S' donor sites prefer Hg^{2+} as predictable from SHAB principle[20]. Literature reports suggest that nature and length of the spacer in different rhodamine conjugates control its selectivity for different analytes, for example, use of hydrazine and ethylenediamine as spacer have marked difference towards metal ion selectivity.[21,22] The synthetic protocol of RSQ is shown in Scheme 1. All the intermediates have been characterised by ^{1}H NMR, ^{13}C NMR and QTOF-MS spectra (Figure S-1 to S-9, ESI†).

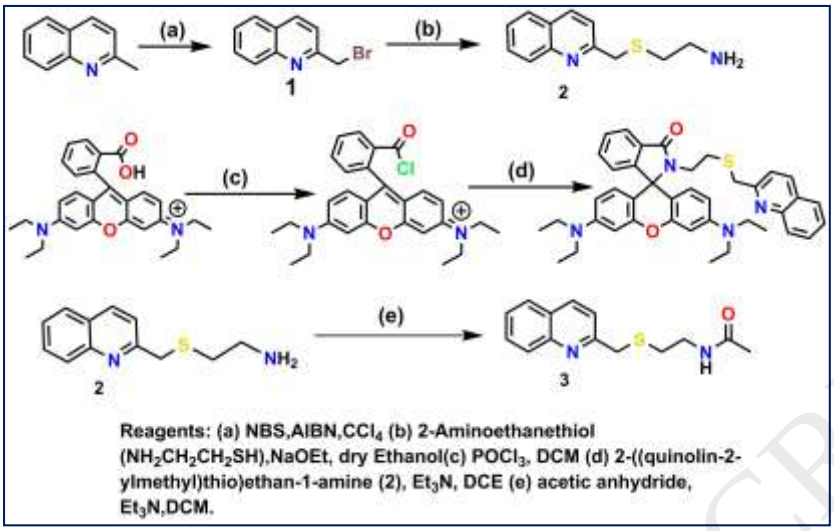

Scheme 1 Synthetic route to **RSQ**

3.1. Photo-physical studies

Solvent plays an important role to the selectivity of rhodamine based probes for different analyte. In present case, DMSO: water (1:1, v/v) was used as working solvent for selective detection of Bi^{3+} ion. Initially, higher percentage of water (DMSO: water, 1: 4, v/v) was used for detection of Bi^{3+} ion because of highest emission intensity for Bi^{3+} was observed in this media. Unfortunately, at higher water content of the media, Hg^{2+} interfere to some extent which may be eliminated using masking agent like $I^-/S^{2-}/NCS^-$.[16,23] However, both I^- / S^{2-} masks Bi^{3+} to form insoluble BiI_3/ Bi_2S_3. Hence, NCS^- is chosen which had no adverse effect on the emission intensity of **RSQ** or **RSQ**-Bi^{3+} systems (Figure 1). However, at low water percentage (DMSO: water, 1:1, v/v), interference from Hg^{2+} ion is insignificant and hence chosen this media for entire studies (Figure S-10, ESI†).

The fluorescence response of **RSQ** towards Bi^{3+} in presence of other cations was presented in Figure S-11 (ESI†). Figure 2 show the selectivity of **RSQ** (λ_{em} = 597 nm; λ_{ex} =525 nm) for common cations while the inset presents corresponding colour changes.

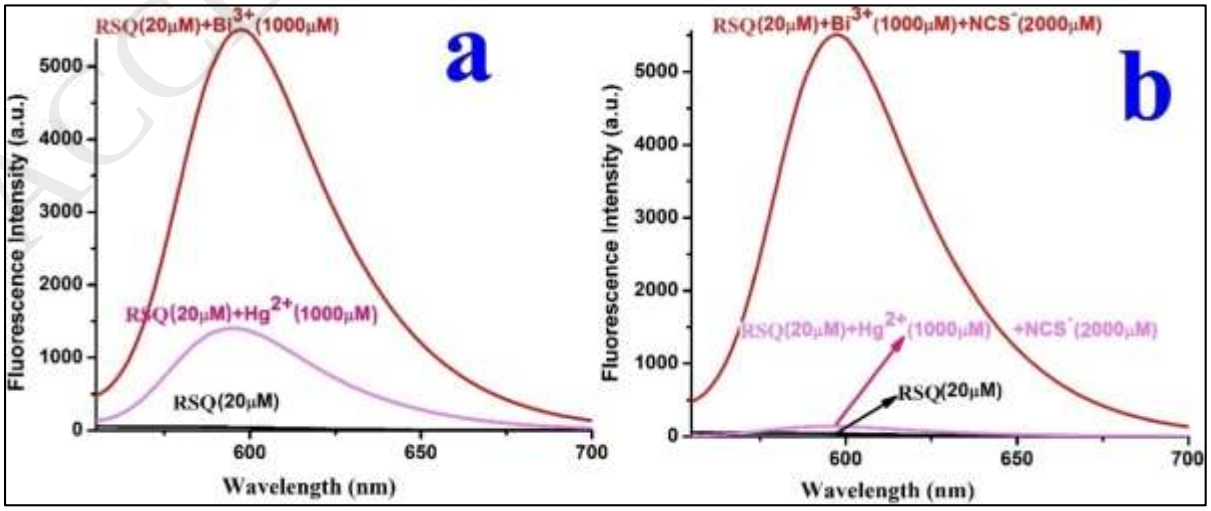

Figure 1 Fluorescence spectra of **RSQ** (20 μM) (a) in presence of Hg^{2+} (1000 μM) and Bi^{3+} (1000 μM); (b) upon addition of NCS^{-} (2000 μM) to the system shown in (a); Medium: HEPES buffer (0.1 M, pH 7.4), DMSO: water (1:1, v/v) (λ_{ex}, 525 nm)

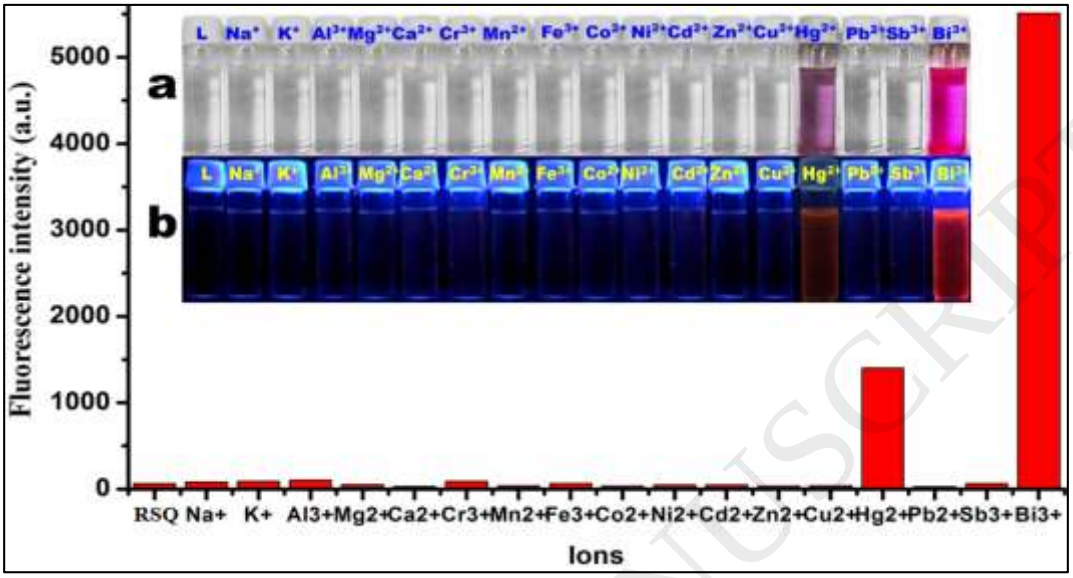

Figure 2 Emission intensity of **RSQ** (20 μM) at 597 nm (λ_{ex}, 525 nm) in presence of different cations (1000 μM) in mentioned media; Inset: colours upon irradiation with (a) visible and (b) UV light

The UV-vis. spectrum of **RSQ** exhibited an absorption band centered at 322 nm (Figure 3). Figure 3A show changes of absorption spectra in presence of common cations, mentioned in Figure 2.

Initially, absorbance at 322 nm increases upon gradual addition of Bi^{3+} up to 1 μM. Further addition of Bi^{3+} (>1 to 1000 μM) gradually decreases this absorbance while a new band that appears at 566 nm gradually increases, indicating spirolactam ring opening of the rhodamine unit (Figure 3B).

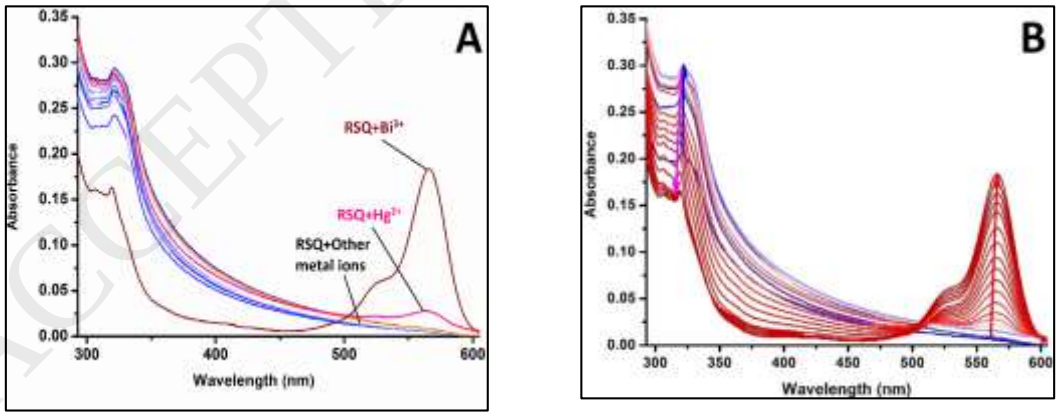

Figure 3 Changes in the UV-Vis. spectra of **RSQ** (20 μM) (A) in presence of different cations (1000 μM) and (B) upon gradual addition of Bi^{3+} (0.0, 0.05, 0.1, 0.5, 1.0, 2.0, 5.0, 10.0, 20.0, 30.0, 50.0, 75.0, 100.0, 150.0, 200.0, 300.0, 500.0, 750.0 and 1000.0 μM) in same media.

Emission of free **RSQ** at 597 nm (λ_{ex} = 525 nm) was very weak (Φ = 0.02) (Figure 4b). In presence of Bi^{3+}, ~130 fold enhancement of emission intensity along with ~30 fold increase of fluorescence

quantum yield ($\Phi = 0.59$) were observed. As two distinct excitation wavelengths *viz.* 365 nm and 525 nm were observed from two emission wavelengths (Figure S-12, ESI†), fluorescence titration was carried out at both wavelengths (Figure 4a and 4b). **RSQ** show emission at 450 nm upon excitation at 365 nm, characteristics of quinoline emission whereas the emission at 597 nm was due to open ring spirolactam form of rhodamine unit. The emission intensity at 450 nm increases up to 1μM Bi^{3+} and then decreases gradually up to 1000 μM Bi^{3+} while the emission intensity at 597 nm increases continuously upon addition of Bi^{3+} (Figure 4a). On the other hand, changing the excitation wavelength to 525 nm changes the emission profile of the same system as presented in Figure 4b. Figure 4d shows the plot of respective emission intensity *vs.*Bi^{3+} concentration (λ_{em}, 597 nm, λ_{ex}, 525 nm). Lowest concentration of Bi^{3+} detected by **RSQ** is 0.05 μM. The effect of pH on **RSQ** in presence and absence of Bi^{3+} was presented in Figure S-13 (ESI†). Gradual change of the colour of **RSQ** with increasing Bi^{3+} concentration was shown in Figure S-14 (ESI†). Addition of Bi^{3+} (up to 1μM) enhanced the emission intensity at 450 nm, ascribed as CHEF process (λ_{ex}, 365 nm) involving quinoline unit. To further strengthen the CHEF process, a model compound, 3 devoid of rhodamine unit was synthesized (Scheme 1) that had emission maxima centered at 450 nm. Upon addition of Bi^{3+} ion, its emission maxima red shifted to 503 nm (Figure S-18, ESI) due to CHEF process involving quinoline unit. It is proposed that at low concentration (<1μM), Bi^{3+} interact solely with quinoline moiety whereas at higher concentration (>1μM), the spirolactam ring of rhodamine unit opens and consequently, emission at 597 nm increases significantly along with gradual decrease of quinoline band, indicating the commencement of FRET process. Thus the present probe recognizes Bi^{3+} through CHEF assisted FRET process[16,23] where quinoline unit is FRET donor and open ring rhodamine unit is FRET acceptor.[16] Figure 4c show significant overlap between donor emission (quinoline) and acceptor absorbance (open ring rhodamine B), a basic criterion for FRET process. From Job's plot (Figure S-15, ESI†), 1:1 stoichiometry between **RSQ** and Bi^{3+} was established. The binding constant of **RSQ** for Bi^{3+} is 2.1×10^5 (Figure S-16, ESI†).

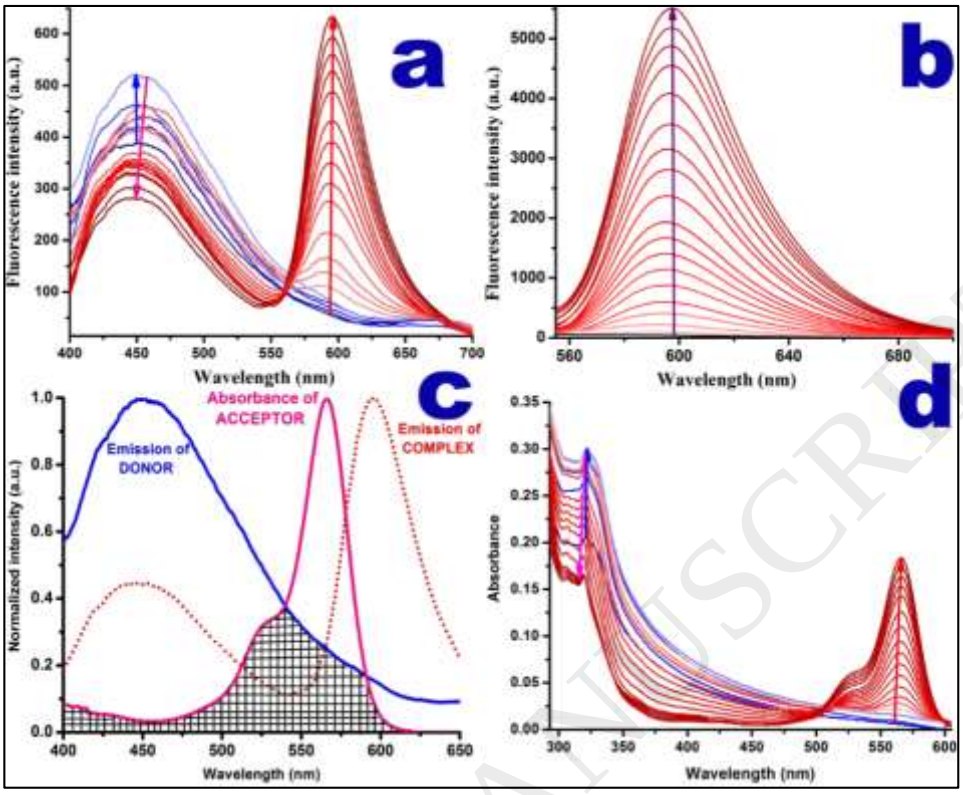

Figure 4 Changes in the emission spectra of **RSQ** (20 μM) upon gradual addition of Bi^{3+} (0.0, 0.05, 0.1, 0.5, 1.0, 2.0, 5.0, 10.0, 20.0, 30.0, 50.0, 75.0, 100.0, 150.0, 200.0, 300.0, 500.0, 750.0 and 1000.0 μM) (a) λ_{ex}, 365 nm and (b) λ_{ex}, 525 nm; (c) spectral overlap between donor emission (quinoline; blue) and acceptor absorbance (open ring rhodamine B; pink). The dotted line (red) shows the emission spectrum of adduct [**RSQ** + Bi^{3+}] and (d) emission intensity *vs.* Bi^{3+} concentration at 597 nm (λ_{ex}, 525 nm).

3.2. ^{1}H NMR titration

To unveil the sensing mechanism, ^{1}HNMR titration was performed. Changes in the ^{1}HNMR signal of **RSQ** in presence of Bi^{3+} were presented in Figure 5. Protons of rhodamine moiety (marked as f, g, h, i, o, j and p) were shifted downfield significantly (marked as f´, g´, h´, i´, o´ and p´). The 'j' proton was shifted up-field to j´. The protons of quinoline unit marked as k, l, n, q and r were downfield shifted to k´, l´, n´, q´ and r´ and m was up-field shifted to m´ in presence of Bi^{3+}. Mass spectrum (Figure S-17, ESI†) also confirmed the formation of the [**RSQ** + Bi^{3+}] adduct having m/z at 485.6365.

3.3. Theoretical studies

DFT studies theoretically support Bi^{3+} assisted FRET ON process. The optimized geometries of **RSQ** (Table S-1, ESI†) and **RSQ**+Bi^{3+} (Table S-2, ESI†) were generated using 6-31G/LanL2DZ and B3LYP/LanL2DZ basis sets, respectively with Gaussian 09 software[24]. The HOMO-LUMO energy differences of [**RSQ**+Bi^{3+}] adduct was lower than that of free **RSQ** (Figure S6). Indicating formation of stable adduct by **RSQ** with Bi^{3+} ion.

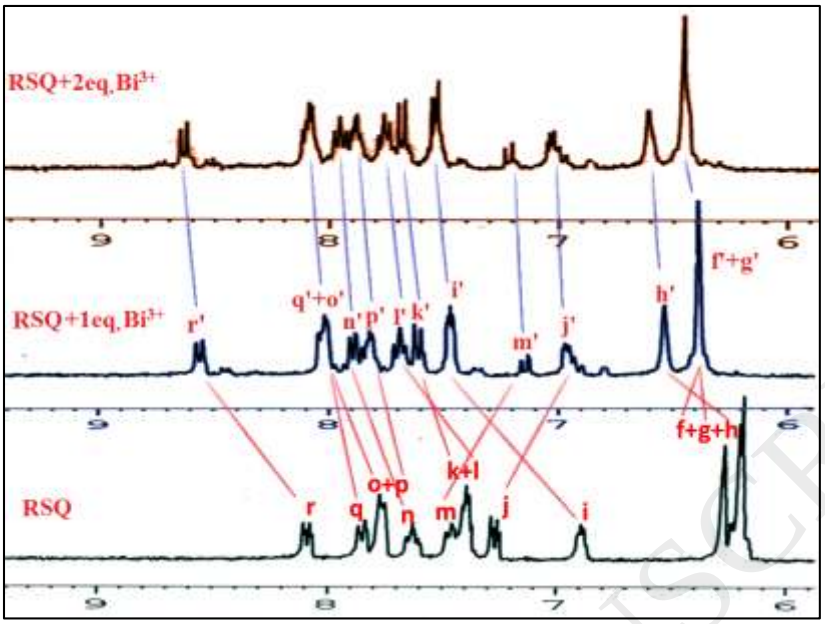

Figure 5 ^{1}HNMR titration: (I) free **RSQ**; (II) **RSQ** + 1.0 equiv. Bi^{3+}; (III) **RSQ** + 2.0 equiv. Bi^{3+} in methanol-d_4

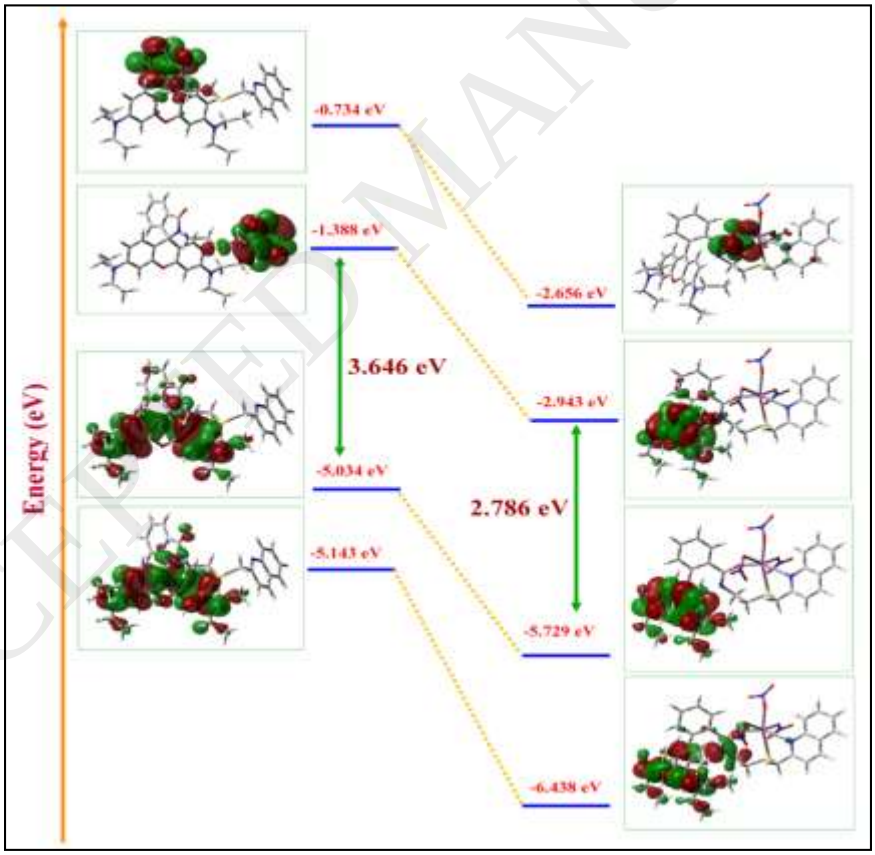

Figure 6 HOMO-LUMO energy difference of free **RSQ** and [**RSQ**+Bi^{3+}] adduct

Considering all these facts, the possible sensing mechanism was portrayed in Figure 7. The increase of absorbance and fluorescence of quinoline unit at lower Bi^{3+} concentration probably indicated predominant **RSQ**: Bi^{3+} = 2:1 (mole ratio) interaction. At higher Bi^{3+} concentration, **RSQ**: Bi^{3+} mole ratio

switched to 1:1 while the spirolactam ring of rhodamine opens to initiate the FRET process, consequently quinoline emission decreases. Lack of optical probes for selective recognition of Bi^{3+} ion forced us to compare the present method with other reported methods for Bi^{3+} detection (Table S-3, ESI†).

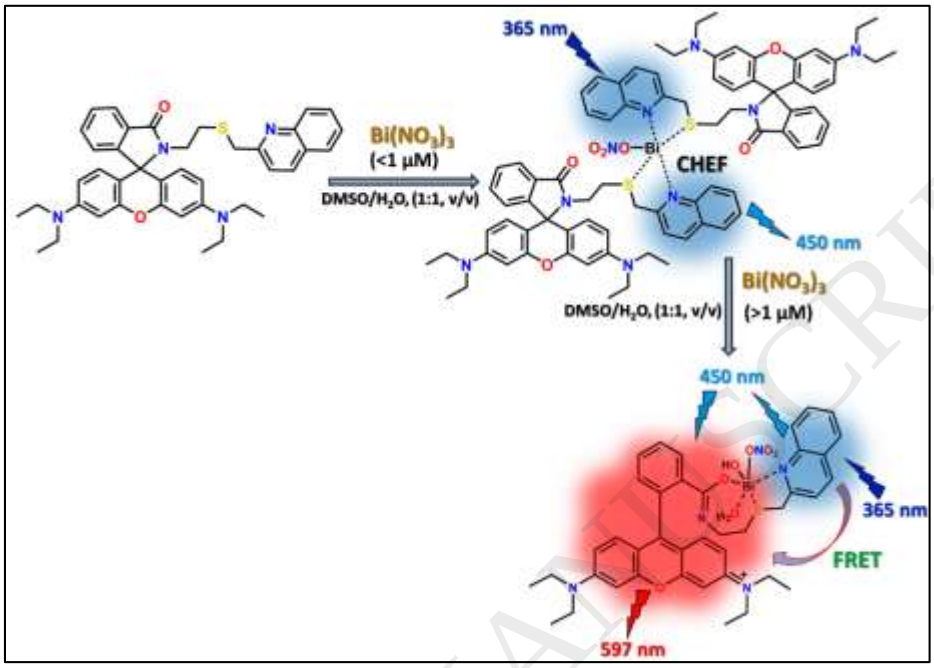

Figure 7 Probable sensing mechanism of RSQ with Bi^{3+}

3.4. Cell imaging studies

Although no cytotoxic effect of Bi^{3+} is established so far, yet RSQ was explored to detect intracellular Bi^{3+}, for any possible biological applications. It is important to note that several thiol containing biogenic moieties are present inside the cell. The thiophilic character of Bi^{3+} ion may tend to form stable complex with this bio-molecules. However, the concentration of these bio-molecules being low, free intra-cellular Bi^{3+} ion may be detected using the present probe. Cells were incubated at 37^0C and 5% CO_2 in culture medium. The cells were incubated in presence and absence of 20 μM **RSQ** for 2h. Then the cells were washed thrice with PBS buffer followed by addition of 50 μM Bi^{3+} to the medium. Fluorescence images of the cells were obtained using an EVOS® FL Cell Imaging System, Life Technologies, USA). Figure 8 show that **RSQ** emits red fluorescence in presence of intracellular Bi^{3+} ion. The control experiment with cells incubated with only Bi^{3+} ion shows no cytotoxic effect.

The cytotoxicity of **RSQ** on SiHa cells was determined by MTT assay (Figure S-19, ESI†). Upon exposure of 20 μM **RSQ** for 12h, ~90% of the cells remains viable. This nullifies the possibility of any significant cytotoxic influence of **RSQ** on SiHa cells. Therefore, **RSQ** may be used as an effective chemosensor for Bi^{3+} in living systems.

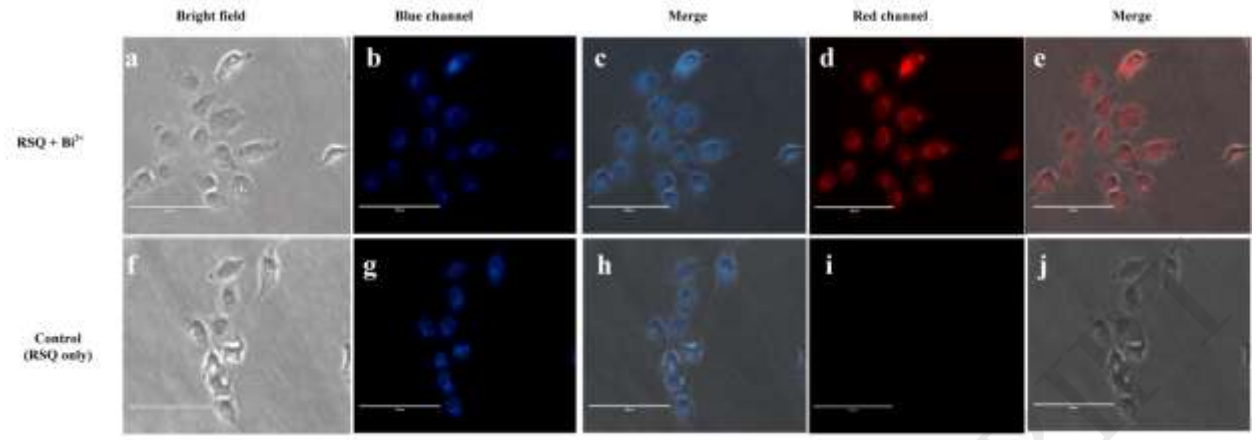

Figure 8 Imaging of Bi^{3+} in SiHa cells: (a) bright field image of cells after incubating 10 μM **RSQ** with 50 μM Bi^{3+}; (b) fluorescence image of the cells in blue channel; (c) are merge images of a and b ; (d) fluorescence image of the cells in red channel; (e) merge images of a and d; (f) Bright field images of control cells after incubating only with 10 μM **RSQ;** (g) fluorescence image of the cells; (h) merge images of cells f and h; (i) fluorescence images under red channel; (j) merge images of cells f and i; **RSQ** was prepared in 0.3% DMSO in water. [Blue channel: 360 nm excitation, 447 nm emission; red channel: 530 nm excitation, 593 nm emission;]

Figure 8 reveals that **RSQ** is cell permeable to efficiently image intracellular Bi^{3+} in live SiHa cells under fluorescence microscope.

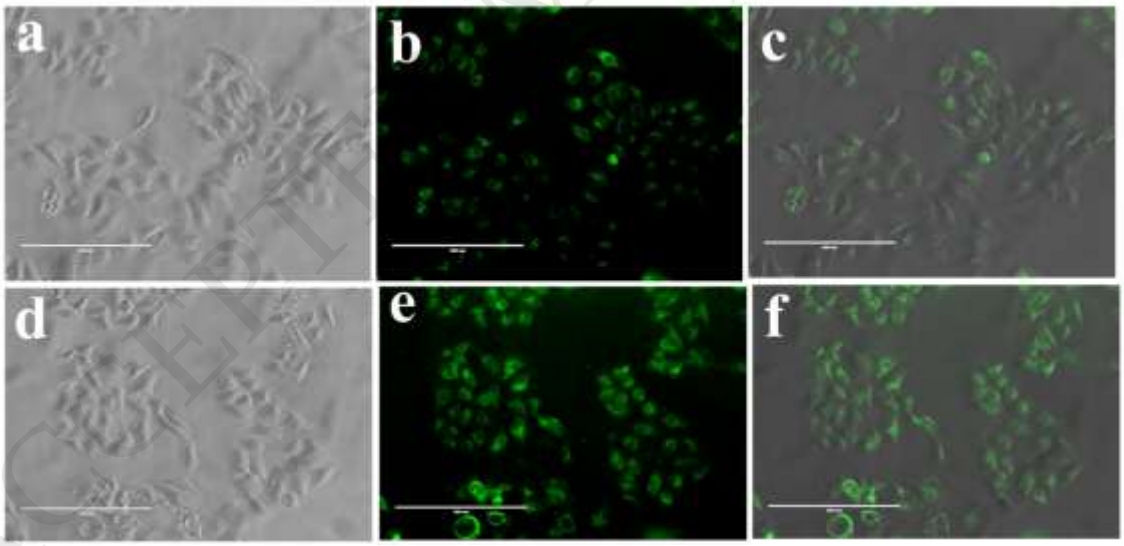

Figure 9 Imaging of Bi^{3+} in HeLa cells: (a) bright field image of cells after incubating with 10 μM **3**; (b) fluorescence image of the cells in green channel; (c) are merge images of a and b ; (d) Bright field images of cells after incubating with 10 μM **3** and followed by 10 μM Bi^{3+}; (e) fluorescence image of the cells; (f) merge images of cells d and e. [green channel: 470 nm excitation, 525 nm emission]

Figure 9 shows that upon addition of Bi^{3+} ion, the fluorescence intensity of 3 in live cell also increase to 10 fold. Therefore, the observed CHEF process predicted for RSQ should be attributed from the initial binding of Bi^{3+} ion with amine compound 2 present in RSQ.

Conclusion

In summary, we have demonstrated a FRET based rhodamine-quinoline conjugate (**RSQ**) as an excellent chemo-sensor for selective detection of Bi^{3+}. **RSQ** changes its colour and fluorescence property upon addition of Bi^{3+}. The LOD of **RSQ** for Bi^{3+} is 0.05 μM, obtained by fluorescence method. **RSQ** can efficiently images intra cellular Bi^{3+} in SiHa cell line.

5. References

1. (a) J. Li, L. Jiang, B. Wang, F. Liu, J. Yang, D. Tang, Y. Lai, J. Li, Electro deposition and characterization of copper bismuth selenide semiconductor thin films, Electrochim. Acta 87 (2013) 153–157; (b) M. A. Berding, A. Sher, A.B. Chen, W. E. Miller, Structural properties of bismuth-bearing semiconductor alloys, J. Appl. Phys. 63 (1988) 107-115.

2. (a) M. Fickling, Review of bismuth in 1998, Bull. Bismuth Inst. 74 (1999) 3-4; (b) K. Michalke, A. Schmidt, B. Huber, J. Meyer, M. Sulkowski, A. V. Hirner, J. Boertz, F. Mosel, P. Dammann, G. Hilken, H. J. Hedrich, M. Dorsch, A. W. Rettenmeier, R. Hensel, Role of Intestinal Microbiota in Transformation of Bismuth and Other Metals and Metalloids into Volatile Methyl and Hydride Derivatives in Humans and Mice, Appl. Environ. Microbiol. 74 (2008) 3069–3075.

3. A. Silkkerveer, F. A. de Wolff, Pharmacokinetics and Toxicity of Bismuth Compounds, Med. Toxicol. Adverse Drug Exper. 4 (1989) 303-323; (b) G. G. Briand, N. Burford, Bismuth Compounds and Preparations with Biological or Medicinal Relevance,Chem. Rev. 99 (1999) 2601-2658; (c) H. Menge, M. Gregor, B. Brosius, R. Hopert, A. Lang,Pharmacology of bismuth, Eur. J. Gastroenterol. Hepatol. 4 (1994) 41-47; (d) H. Sun, H. Li, I. Harvey, P. J. Sadler, Interactions of Bismuth Complexes with Metallothionein (II), J. Biol.Chem. 274 (1999), 29094–29101; (e) L. Zhang, K. Y. Szeto, W. B. Wong,T. T. Loh, P. J. Sadler, H. Sun,Interactions of Bismuth with Human Lactoferrin and Recognition of the Bi^{III}–Lactoferrin Complex by Intestinal Cells,Biochemistry 40 (2001) 13281-13287.

4. M. Wada, K. Akiba, Metallic bismuth mediated allylation of aldehydes to homoallylic alcohols, Tetrahedron Lett. 26 (1985) 4211-4212.

5. A. K. Das, R. Chakraborty, M. L. Cervera, M. de la Guardia, Analytical techniques for the determination of bismuth in solid environmental samples,Trac-Trend Anal. Chem. 25 (2006) 599–608.

6. N. Tokman, S. Akman, Determination of bismuth and cadmium after solid-phase extraction with chromosorb-107 in a syringe, Anal. Chim. Acta 519 (2004) 87-91.

7. G. G. Briand, N. Burford, Bismuth Compounds and Preparations with Biological or Medicinal Relevance, Chem. Rev. 99 (1999) 2601-2658.

8. R. Pamphlett, M. Stottenberg, J. Rungby, G. Danscher, Uptake of bismuth in motor neurons of mice after single oral doses of bismuth compounds, Neuro-toxicol. Teratol. 22 (2000) 559-563.

9. (a) M. Burguera, J. L. Burguera, C. Rondon, M. I. Garcia,Y. P. de Peña, L. M. Villasmil, Determination of bismuth in biological tissues by electrothermal atomic absorption spectrometryusing platinum and tartaric acid as chemical modifier, J. Anal. At. Spectrom. 16 (2001) 1190-1195; (b) P. Y. Sedeño, J. M. Pingarrón, L. Hernández, Handbook of green analytical-chemistry, Ch 14, Wiley, New York(2012) 261; (c) R. Mohan, Green bismuth, Nat. Chem. 2 (2010) 336; (d) A. J. Moghimi, Pre concentration of Ultra Trace Amounts Bismuth in Water Samples Using Cloud Point Extraction with Na-DDTC and Determination by Electro thermal Atomic Absorption Spectrometry (ET-AAS), Korean Chem. Soc. 52 (2008) 140-147; (e) J. Kearns, A. Turner,An evaluation of the toxicity and bioaccumulation of bismuth in the coastal environment using three species of macro alga, Environ. Pollut. 208 (2016) 435-441; (f) I. Švancara, C. Prior, S. B. Hocevar, J. Wang, A Decade with Bismuth-Based Electrodes in Electroanalysis, Electroanalysis 22 (2010) 1405-1420.

10. (a) W. Chen, S. Jiang, Y. Chen, A. C. Sahayam, Slurry sampling flow injection chemical vapor generation inductively coupled plasma mass spectrometry for the determination of trace Ge, As, Cd, Sb, Hg and Bi in cosmetic lotions, Anal.Chim. Acta 860 (2015) 8-14; (b) K. Norisuye, Y. Sohrin, Determination of bismuth in open ocean waters by inductively coupled plasma sector-field mass spectrometry after chelating resin column preconcentration, Anal. Chim. Acta 727 (2012) 71-77; (c) L. Abranko, Z. Stefanka, P. Fodor, Possibilities and limits of the simultaneous determination of As, Bi, Ge, Sb, Se, and Sn by flow injection–hydride generation–inductively coupled plasma–time-of-flight mass spectrometry (FI–HG–ICP–TOFMS), Anal. Chim. Acta 493 (2003) 13-21.

11. (a) H. Matusiewicz, M. Krawczyk, Determination of trace amounts of bismuth by in situ trapping hydride generation flame atomic absorption spectrometry, Chem. Anal. 52 (2007) 565; (b) Z. Li, Y. Guo,Simultaneous determination of trace arsenic, antimony, bismuth and selenium in biological samples by hydride generation-four-channel atomic fluorescence spectrometry, Talanta 65 (2005) 1318-1325.

12. T. Madrakian, A. Afkhami, A. Esmaeili,Spectrophotometric determination of bismuth in water samples after preconcentration of its thiourea–bromide ternary complex on activated carbon,Talanta 60 (2003) 831-838; (b) P. C. A. Jerónimo, A. N. Araújo, M. C. Montenegro, D. Satinský, P. Solich, Colorimetric bismuth determination in pharmaceuticals using a xylenol orange sol–gel sensor coupled to a multicommutated flow system, Anal. Chim. Acta 504 (2004) 235-241; (c) A. Niazi, S. Habibi, M. Ramezani, spectrophotometric determination of bismuth in water samples by dispersive liquid-liquid microextraction after multivariate optimization based on box-behnken, J. Chil. Chem. Soc. 58 (2013) 1899-1901.

13.F. Cui, L. Wang, Y. Cui, Determination of bismuth in pharmaceutical products using methyltriphenyl phosphonium bromide as a molecular probe by resonance light scattering technique, J. Pharm. Biomed. Anal. 43 (2007) 1033-1038.

14.(a) J. Zen, M. Chung,Square-wave voltammetric stripping analysis of bismuth(III) at a poly(4-vinylpyridine)/mercury film electrode,Anal. Chm. Acta 320 (1996) 43-51; (b) F. Fathirad, D. Afzali, A. Mostafavi,

T. Shamspur, S. Fozooni, Fabrication of a new carbon paste electrode modified with multi-walled carbon nanotube for stripping voltammetric determination of bismuth(III), Electro-chim. Acta 103 (2013) 206-210; (c) M. B. Gholivand, A. A. Romiani, Application of adsorptive stripping voltammetry to the simultaneous determination of bismuth and copper in the presence of nuclear fast red, Anal. Chim. Acta 571 (2006) 99-104; (d) H. Guo, Y. Li, P. Xiao, N. He, Determination of trace amount of bismuth (III) by adsorptive anodic stripping voltammetry at carbon paste electrode, Anal.Chim. Acta 534 (2005) 143-147; (e) K. L. Dong, L. Kryger, J. K. Christensen, K. N. Thomsen,Preconcentration and determination of Bismuth (III) at a chemically modified electrode containing 1-(2-pyridylazo)-2-naphthol,Talanta 38 (1991) 101-105; (f) H. Yang, W. Chen, I. Sun,Anodic stripping voltammetric determination of bismuth(III) using a Tosflex-coated mercury film electrode, Talanta 50 (1999) 977-984; (g) S. S. Khaloo, A. A. Ensafi, T. Khayamian,Determination of bismuth and copper using adsorptive stripping voltammetry couple with continuous wavelet transform, Talanta 71 (2007) 324-332; (h) A. Koper, M. Grabarczyk,Electrochemical determination of bismuth with use of a Bi(III)-cupferron complexation system and elimination of interferences connected with the presence of organic substances in natural samples, J. Electroanal. Chem. 663 (2011) 67-71.

15.(a) S. Mandal, A. Banerjee, S. Lohar, A. Chattopadhyay, B. Sarkar, S. K. Mukhopadhyay, A. Sahana, D. Das, Selective sensing of Hg^{2+} using rhodamine-thiophene conjugate: red light emission and visual detection of intracellular Hg^{2+} at nanomolar level,J. Hazard. Mater. 261 (2013) 198-205; (b) S. Mandal, A. Banerjee, D. Ghosh, D. K. Mandal, D. A. Safin, M. G. Babashkina, K. Robeyns, M. P. Mitoraj, P. Kubisiak, Y. Garcia, D. Das, An anion induced multisignaling probe for Hg^{2+} and its application for fish kidney and liver tissue imaging studies,Dalton Trans. 44 (2015) 13186-13195; (c) S. Mandal, A. Sahana, A. Banerjee, D. A. Safin, M. G. Babashkina, K.Robeyns, S. Verkaart, J. G. J. Hoenderop, M. P. Mitoraj, Y. Garcia, D. Das, A smart rhodamine–pyridine conjugate for bioimaging of thiocyanate in living cells, RSC Adv. 5 (2015) 103350-103357; (d) S. Nandi, A. Sahana, S. Mandal, A.Sengupta, A. Chatterjee, D. A. Safin, M. G. Babashkina,N. A. Tumanov, Y. Filinchuk, D. Das,Hydrazine selective dual signaling chemodosimetric probe in physiological conditions and its application in live cells, Anal. Chim. Acta 893 (2015) 84-90; (e) S. Adhikari, S. Mandal, A. Ghosh, S. Guria, D. Das, Tuning of donor-acceptor linker in rhodamine-coumarin conjugates leads remarkable solvent dependent FRET efficiency for Al^{3+} imaging in HeLa cells, Sensor. Actuat. B: Chem. 234 (2016) 222-230; (f) X. Zhang, Y. Xiao, X. Qian,A ratiometric fluorescent probe based on FRET for imaging Hg^{2+} ions in living cells,Angew. Chem. Int. Ed. 47 (2008) 8025-8029; (g) M. Beija, C. A. M. Afonso, J. M. G. Martinho,Synthesis and applications of Rhodamine derivatives as fluorescent probes,Chem. Soc. Rev. 38 (2009) 2410-2433; (h) M. Savarese, A. Aliberti, I. De Santo, E. Battista, F. Causa, P. A. Netti, N. Rega, Fluorescence Lifetimes and Quantum Yields of Rhodamine Derivatives: New Insights from Theory and Experiment, J. Phys. Chem. A 116 (2012) 7491-7497; (i) Y. Q. Sun, J. Liu, X. Lv, Y. Liu, Y. Zhao, W. Guo,Rhodamine-Inspired Far-Red to Near-Infrared Dyes and Their Application as Fluorescence Probes,Angew. Chem. Int. Ed. 51 (2012) 7634-7636; (j) A. Banerjee, A. Sahana, S. Lohar, I. Hauli,S. K.Mukhopadhyay, D. A. Safin, M. G. Babashkina,M. Bolte, Y. Garcia, D. Das,A rhodamine derivative as a “lock” and SCN^- as a “key”: visible light excitable SCN^- sensing in living cells, Chem. Commun. 49 (2013) 2527-2529.

16. S. Adhikari, S. Mandal, A. Ghosh, P. Das, D. Das, Strategically Modified Rhodamine–Quinoline Conjugate as a CHEF-Assisted FRET Probe for Au^{3+}: DFT and Living Cell Imaging Studies, J. Org. Chem. 80 (2015) 8530-8538.

17. (a) N. Wei, N. N. Murthy, Q. Chen, J. Zubieta, K. D. Karlin, Copper(I)/Dioxygen Reactivity of Mononuclear Complexes with Pyridyl and Quinolyl Tripodal Tetradentate Ligands: Reversible Formation of $Cu:O_2$ = 1:1 and 2:1 Adducts, Inorg. Chem. 33 (1994) 1953-1965; (b) S. Zahn, D. Das, J. W. Canary, Redox-Induced Ligand Reorganization and Helicity Inversion in Copper Complexes of *N*, *N*-Dialkylmethionine Derivatives, Inorg. Chem. 45 (2006) 6056-6063; (c) J. Huang, Y. Xu, X. Qian, A Rhodamine-Based Hg^{2+} Sensor with High Selectivity and Sensitivity in Aqueous Solution: A NS_2-Containing Receptor, J. Org. Chem. 74 (2009) 2167-2170.

18.(a) P. Domenico, R. J. Salo, S. G. Novick, P. E. Schoch, K. van Horn, B. A. Cunha,Enhancement of bismuth antibacterial activity with lipophilic thiol chelators, Antimicrob. Agents Chemother. 41 (1997) 1697-1703; (b) H. Li, H. Sun,Recent advances in bioinorganic chemistry of bismuth, Curr. Opin. Chem. Biol. 16 (2012) 74-83.

19. (a) M. Beija, C. A. M. Afonso, J. M. G. Martinho, Synthesis and applications of Rhodamine derivatives as fluorescent probes, Chem. Soc. Rev. 38 (2009) 2410-2433; (b) A. Gupta, N. Kumar,A review of mechanisms for fluorescent ‘‘turn-on’’ probes to detect Al^{3+} ions, RSC Adv. 6 (2016) 106413-106434.

20. (a) T. L. Ho, Hard soft acids bases (HSAB) principle and organic chemistry, Chem. Rev. 75 (1975) 1-20; (b) Q. Mei, L. Wang, B. Tian, F. Yan, B. Zhang, W. Huang, B. Tong,A highly selective and naked-eye sensor for Hg^{2+}based on quinazoline-4(3H)-thione,New J. Chem. 36 (2012) 1879-1883; (c) S. Park, W. Kim, K. M. K. Swamy, H. Y. Lee, J. Y. Jung, G. Kim, Y. Kim, S. J. Kim, J. Yoon, Rhodamine hydrazone derivatives bearing thiophene group as fluorescent chemosensors for Hg^{2+}, Dyes Pigments 99 (2013) 323–328.

21. (a) S. Samanta, T. Ray, F. Haque, G. Das, A turn-on Rhodamine B-indole based fluorogenic probe for selective sensing of trivalent ions, J. Lumin. 171 (2016) 13-18; (b) C. Kar, M. D. Adhikari, A. Ramesh, G. Das,NIR- and FRET-Based Sensing of Cu^{2+} and S^{2-} in Physiological Conditions and in Live Cells, Inorg. Chem. 52 (2013) 743-752.

22. (a) K. N. Kim, M. G. Choi, J. H. Noh, S. Ahn, S. K. Chang, Rhodamine B hydrazide revisited: chemodosimetric Hg^{2+}-selective signaling behavior in aqueous environments, Bull. Korean Chem. Soc. 29 (2008) 571-574; (b) P. Praikaew, T. Duangdeetip, N. Chimpalee, C. Wainiphithapong, P. Swanglap and N. Wanichacheva, Colorimetric sensor for detection of Hg^{2+} in aqueous samples utilizing rhodamine B hydrazide modified silica, Mater. Express 5 (2015) 300-308; (c) C. R. Lohani, J. M. Kim, S. Y. Chung, J. Yoon, K. H. Lee, Colorimetric and fluorescent sensing of pyrophosphate in 100% aqueous solution by a system comprised of rhodamine B compound and Al^{3+}complex, Analyst 135 (2010) 2079-2084.

23. A. Sahana, A. Banerjee, S. Lohar, B. Sarkar, S. K. Mukhopadhyay, D. Das,Rhodamine-Based Fluorescent Probe for Al^{3+} through Time-Dependent PET–CHEF–FRET Processes and Its Cell Staining Application, Inorg. Chem. 52 (2013) 3627-3633.

24. M. J. Frisch, G. W. Trucks, H. B. Schlegel, G. E. Scuseria, M. A. Robb, J. R. Cheeseman, G. Scalmani, V. Barone, B. Mennucci, G. A. Petersson, H. Nakatsuji, M. Caricato, X. Li, H. P. Hratchian, A. F. Izmaylov, J. Bloino, G. Zheng, J. L. Sonnenberg, M. Hada, M. Ehara, K. Toyota, R. Fukuda, J. Hasegawa, M. Ishida, T. Nakajima, Y. Honda, O. Kitao, H. Nakai, T. Vreven, J. A. Montgomery Jr., J. E. Peralta, F. Ogliaro, M. Bearpark, J. J. Heyd, E. Brothers, K. N. Kudin, V. N. Staroverov, R. Kobayashi, J. Normand, K. Raghavachari, A. Rendell, J. C. Burant, S. S. Iyengar, J. Tomasi, M. Cossi, N. Rega, J. M. Millam, M. Klene, J. E. Knox, J. B. Cross, V. Bakken, C. Adamo, J. Jaramillo, R. Gomperts, R. E. Stratmann, O. Yazyev, A. J. Austin, R. Cammi, C. Pomelli, J. W. Ochterski, R. L. Martin, K. Morokuma, V. G. Zakrzewski, G. A. Voth, P. Salvador, J. J. Dannenberg, S. Dapprich, A. D. Daniels, Ö. Farkas, J. B. Foresman, J. V. Ortiz, J. Cioslowski and D. J. Fox, Gaussian 09, Gaussian Inc., Wallingford CT, (2009).